PRAMANA
— journal of
physics

Vol. 79, No. 4
October 2012
pp. 555–562

Quantum chromodynamics effects in electroweak and Higgs physics

FRANK PETRIELLO[1,2]

[1]Department of Physics & Astronomy, Northwestern University, Evanston, IL 60208, USA
[2]High Energy Physics Division, Argonne National Laboratory, Argonne, IL 60439, USA
E-mail: f-petriello@northwestern.edu

Abstract. Several examples of the often intricate effects of higher-order quantum chromodynamics (QCD) corrections on predictions for hadron-collider observables, are discussed, using the production of electroweak gauge boson and the Standard Model Higgs boson as examples. Particular attention is given to the interplay of QCD effects and experimental cuts, and to the use of scale variations as estimates of theoretical uncertainties.

Keywords. Higher-order quantum chromodynamics; electroweak gauge bosons; Higgs physics.

PACS No. 12.38.Bx

1. Introduction

Since its start in 2010, the operation of the Large Hadron Collider (LHC) has been an outstanding success. Roughly 5 fb^{-1} of data was collected by both the ATLAS and CMS experiments by the end of 2011. All major Standard Model (SM) production processes in the electroweak gauge boson and top quark sectors have been re-established, with many measurements already limited by theoretical errors. The remarkable agreement between measurements and predictions for electroweak gauge boson cross-sections ranging over four orders of magnitude is shown by CMS in figure 1.

More importantly, the searches for the Higgs boson predicted by the Standard Model, and for phenomena not explained within our current theoretical framework, have been advanced enormously by the LHC program. After more than a decade of Tevatron Run II data-taking and analysis, the CDF and D0 Collaborations recently announced a combined 95% confidence level (CL) exclusion of the SM Higgs boson in the regions $100\,\text{GeV} \leq m_{\text{H}} \leq 106\,\text{GeV}$ and $147\,\text{GeV} \leq m_{\text{H}} \leq 179\,\text{GeV}$ [2]. Although this result is impressive, the vastly superior reach of the LHC experiments to physics beyond our current understanding is illustrated by the current SM Higgs exclusion plot from ATLAS which is shown in figure 2. In roughly two years of data collection and analysis, the entire mass range $129\,\text{GeV} \leq m_{\text{H}} \leq 539\,\text{GeV}$, together with the smaller windows

DOI: 10.1007/s12043-012-0362-x; ***e*Publication: 27 September 2012**

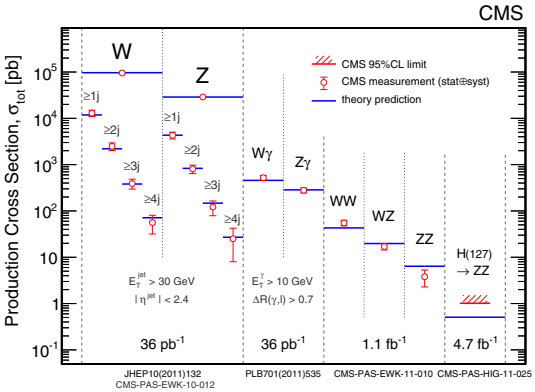

Figure 1. Agreement between CMS measurements and theoretical predictions for W and Z-boson production cross-sections spanning four orders of magnitude, taken from ref. [1].

$110\,\text{GeV} \leq m_\text{H} \leq 117.5\,\text{GeV}$ and $118.5\,\text{GeV} \leq m_\text{H} \leq 122.5\,\text{GeV}$, have been excluded at the 95% CL. Both the Tevatron and LHC experimental collaborations see an excess consistent with a Standard Model Higgs boson with $m_\text{H} \sim 125\,\text{GeV}$, and the 2012 LHC run is eagerly awaited to clarify the situation.

Of course, the SM Higgs boson is not all we hope to find. Numerous arguments point toward a rich theoretical structure revealing itself at the TeV-energy scale being explored at the LHC. The observation of dark matter in the cosmos can be beautifully explained by the WIMP miracle, which posits stable new particles at the TeV scale which manifest themselves as missing energy signatures at the LHC. The large gap between the electroweak and Planck scales can be stabilized by new symmetries such as supersymmetry, which predict numerous new states awaiting discovery. While nothing has yet been

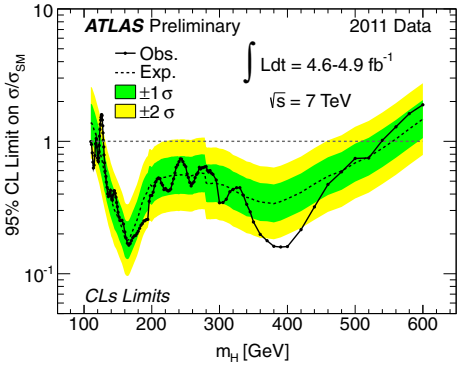

Figure 2. The observed (solid line) and expected (dashed line) 95% CL combined upper limits on the SM Higgs boson production cross-section divided by the Standard Model expectation as a function of m_H [3].

found, the existing exclusion bounds have been significantly strengthened by the LHC data collected so far.

The need for some understanding of QCD in pursuing this program of discovery is obvious. All theoretical predictions rely upon the QCD factorization of perturbative and non-perturbative effects into partonic cross-sections, which can be calculated using perturbative quantum field theory, and parton distribution functions, which must be extracted from measurements. Monte-Carlo event generators are used to model signal and background in every experimental study, while next-to-leading order (NLO) and sometime even next-to-next-to-leading order (NNLO) QCD predictions are needed to make precise, quantitative comparisons between theory and experiment. In many searches for physics beyond the Standard Model, a clear kinematic feature does not distinguish signal from background, and instead an excess of events over SM predictions in the tail of a distribution is searched for. Typical examples are the searches for supersymmetry in the high m_{eff} region in the jets plus missing energy channel, or for the Higgs boson in the $WW \to l\nu l\nu$ channel, as shown in figure 3. Without accurate predictions and a reliable estimate of the residual theoretical errors, no discoveries are possible in these channels.

The intent of this contribution is to illustrate the effect of higher-order QCD corrections on theoretical predictions for LHC processes. These effects are often exacerbated by the chosen experimental cuts, causing sizable corrections to occur in unexpected regions. Large shifts induced by QCD appear near phase-space boundaries, exactly where new physics signatures are expected to occur. Several examples from electroweak gauge boson and Higgs boson production are used to illustrate these points. Methods for setting the renormalization and factorization scales to capture the important higher-order effects and to properly estimate the theoretical uncertainties are also discussed. The available calculations and programs available for calculating higher-order QCD predictions will not be discussed here, as they have been exhaustively reviewed elsewhere [6].

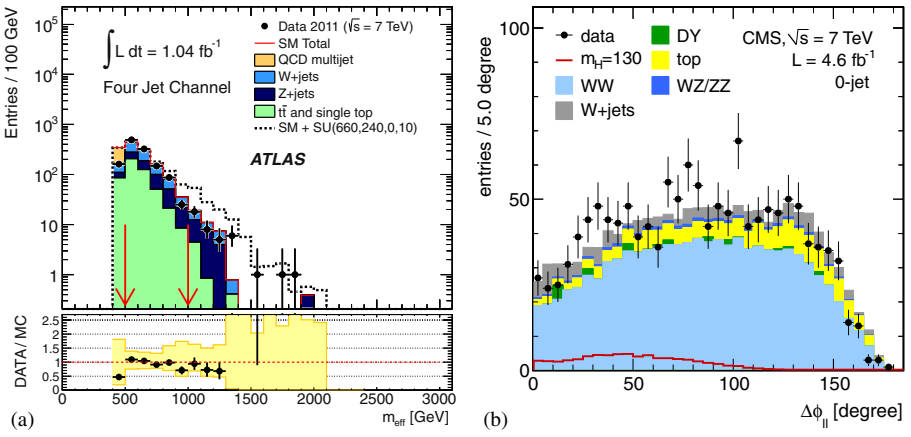

Figure 3. (**a**) Comparison of data, SM backgrounds and a supersymmetric prediction for the m_{eff} distribution in $l\nu + 4$ jets events [4] and (**b**) comparison between Higgs signal and background in the $WW \to ll\nu\nu$ mode [5].

2. The Drell–Yan invariant mass spectrum

The production of lepton pairs, l^+l^-, through intermediate γ^*, Z bosons is a standard candle for LHC physics studies. It is a background to Z' production and numerous other new physics searches. As one of the cleanest processes with copious production, it can be used as a luminosity monitor, to constrain parton distribution functions, and to study electroweak physics parameters. Measurements of inclusive l^+l^- properties at the LHC have already reached the percent-level, and are in several cases limited by theory. The state-of-the-art theoretical predictions for l^+l^- are fully-differential NNLO predictions available in the form of flexible Monte-Carlo integrators [7–9]. Initial steps towards the combination of QCD and electroweak corrections have been taken [10–12].

Improving our knowledge of parton distribution functions is one of the most important uses of the Drell–Yan channel at the LHC. For this purpose it is important to maximize the range of Bjorken-x covered in the measurement. The CMS Collaboration has produced a measurement of the Drell–Yan invariant mass spectrum from $M_{ll} = 15$ GeV to 600 GeV [13], as presented in figure 4. An interesting effect emerges when the lowest invariant mass bin, $15\,\text{GeV} < M_{ll} < 20\,\text{GeV}$, is studied. The event selection in the $\mu^+\mu^-$ channel requires two states with transverse momenta $p_{\text{T1}} > 16$ GeV and $p_{\text{T1}} > 7$ GeV, respectively. Leading-order kinematics for the Drell–Yan process then requires that the invariant mass satisfies $M_{ll} > 23$ GeV, such that the first bin is not populated. Only at higher orders, when the muon pair can recoil against a hard jet, is this lowest bin generated. The standard tool used by CMS to calculate the acceptance in this analysis is POWHEG [14], which generates only one additional hard jet to recoil against the muon pair. This is effectively a leading-order calculation for the $15\,\text{GeV} < M_{ll} < 20\,\text{GeV}$ bin. The POWHEG prediction for this bin is 50% smaller than the NNLO result of FEWZ [8], and not in agreement with the data [13,15]. This delicate interplay between the experimental cuts leads to an underestimate by a large amount of this seemingly innocuous

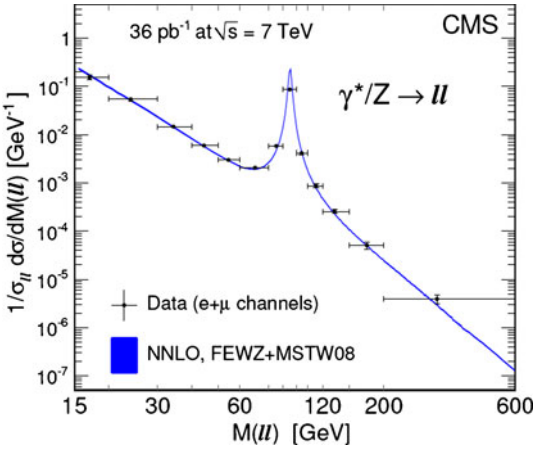

Figure 4. CMS measurement of the Drell–Yan invariant mass spectrum, compared to the NNLO QCD predictions from the program FEWZ.

region of phase space by one of the most advanced NLO+parton shower tools available, and demonstrates both the usefulness of the dedicated higher-order QCD tools to cross-check more general codes, and the need to carefully consider the implications of the chosen acceptance cuts in experimental measurements.

3. The diphoton background in Higgs searches

The primary search channel for a light SM Higgs is through its inclusive production and decay into two photons, $pp \to H \to \gamma\gamma$. The 5 fb^{-1} dataset collected by the ATLAS and CMS Collaborations in 2011 reveals an excess in this mode. Not only is the experimental signature striking, the excellent calorimeter resolutions of the ATLAS and CMS experiments permit a precise determination of the Higgs boson mass. After imposing isolation requirements to remove the large $\pi_0 \to \gamma\gamma$ contamination, the dominant background to this search is the continuum production of photon pairs in perturbative QCD. In their searches the ATLAS and CMS Collaborations utilize 'staggered' cuts on the transverse momenta of the two photons: $p_{\mathrm{T1}} > 40$ GeV and $p_{\mathrm{T1}} > 25$ GeV, respectively [16].

A theoretical study of the $pp \to \gamma\gamma$ background was performed recently using the NLO program MCFM [17]. The impact of QCD corrections was investigated for both the staggered cuts outlined above, and for the symmetric cuts $p_{\mathrm{T1,2}} > 25$ GeV. For symmetric cuts, the increase of the cross-section is roughly 20–30%. The shifts are dramatically large for the staggered cuts used by the experimental collaborations, approaching a factor of three, as shown in figure 5. The theoretical uncertainty as estimated from scale variation also increases when going from LO to NLO. What is happening when staggered cuts are imposed? Note that the leading-order $q\bar{q} \to \gamma\gamma$ and $gg \to \gamma\gamma$ produce photons with equal transverse momenta. The region $25\,\mathrm{GeV} < p_{\mathrm{T1}} < 40\,\mathrm{GeV}$ is only populated at NLO, when the diphoton pair can recoil against a hard gluon. The qg partonic process first opens up at NLO. Because of the cuts and its large luminosity, this channel contributes significantly to the cross-section, as is clear from figure 5. Since it first appears at NLO, it

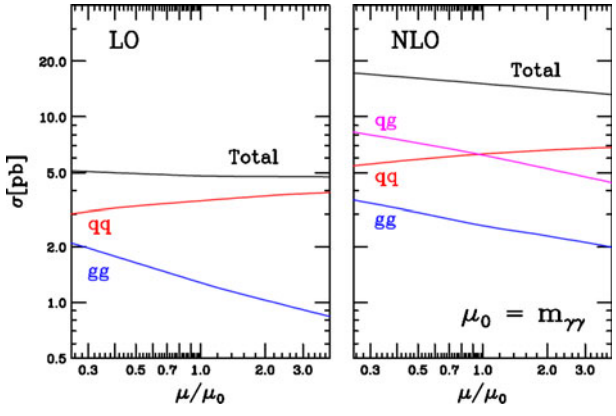

Figure 5. The LO and NLO $pp \to \gamma\gamma$ cross-sections for staggered cuts as a function of the scale μ, obtained using MCFM.

contributes a large-scale variation to the cross-section. In contrast, for symmetric cuts no new phase-space regions opens up at NLO, and the relative importance of the qg channel is reduced, leading to a more convergent perturbative expansion. The better behaviour of symmetric vs. staggered cuts is very observable-specific; for example, symmetric rather than staggered cuts lead to worse convergence for jet production at HERA [18]. A careful study of the observable in question is required to reduce the possible impact of higher-order QCD.

4. The jet veto in gluon-fusion Higgs production

Experimental searches for the Higgs boson in the $H \to WW \to l\nu l\nu$ decay mode typically divide events into bins with either 0, 1 or 2 jets. This is done to maximize the sensitivity to the Higgs signal. Since the background composition changes primarily from continuum WW production in the 0-jet bin to top-pair production in the 2-jet bin, this division allows each exclusive jet bin to be optimized independently to separate the signal from the background. Although preferable from the experimental viewpoint, this complicates theoretical predictions. Vetoing jets to form a 0-jet bin introduces large logarithms into the perturbative expansion. The situation is particularly tricky for the gluon-fusion Higgs cross-section, as discussed in ref. [19]. The large negative corrections from these logarithms cancel large positive corrections to the inclusive cross-section. Not only does this decrease the K-factor in the 0-jet bin, but it also prevents estimating the

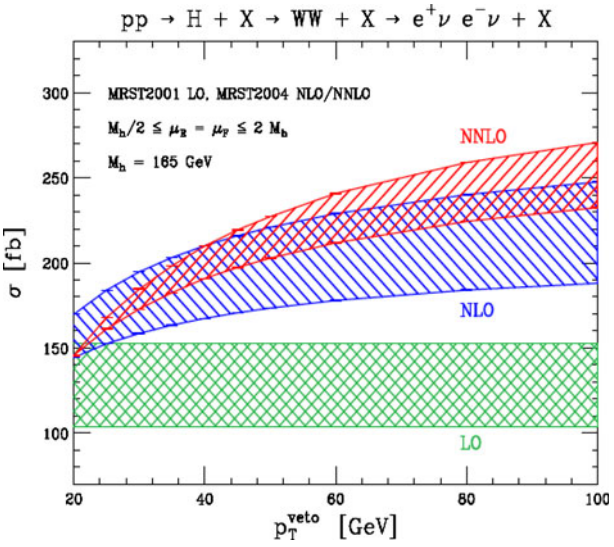

Figure 6. The jet-vetoed cross-section for gluon-fusion Higgs production as a function of the jet cut. The hatched region denotes the theoretical uncertainty estimate obtained by varying the renormalization and factorization scales $\mu_{\rm R} = \mu_{\rm F} = \mu$ by a factor of two around $m_{\rm H}$ (figure taken from ref. [20]).

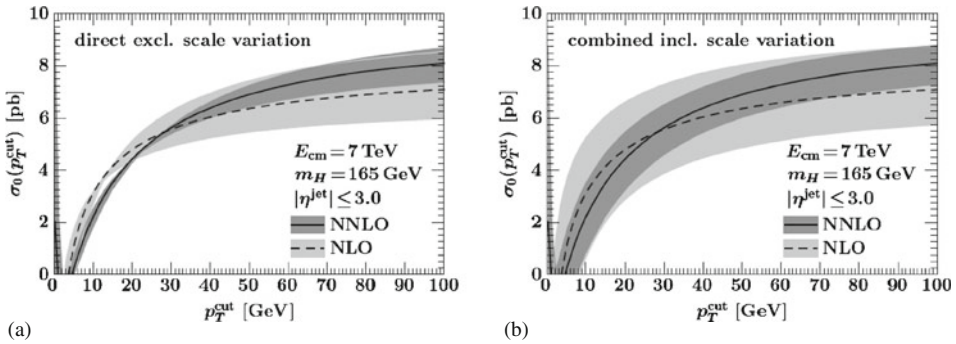

Figure 7. The jet-vetoed cross-section for gluon-fusion Higgs production as a function of the jet cut. The hatched region denotes the theoretical uncertainty estimate obtained by varying the renormalization and factorization scales (**a**) directly in the 0-jet cross-section and (**b**) treating the inclusive 1-jet and total cross-sections as the independent quantities (figure taken from ref. [19]).

theoretical error by directly varying the renormalization and factorization scales in the 0-jet cross-section around a central value. The situation is shown in figure 6, where the error estimate at NNLO approaches zero for $p_{\mathrm{T}}^{\mathrm{veto}} \sim 20$ GeV [20]. Since this small uncertainty results from the accidental cancellation of two independent series, it is not indicative of the potential size of the missing higher-order terms.

A remedy to properly estimate the residual theoretical uncertainty was suggested in ref. [19]. It was pointed out that in the limit that the jet-veto logarithm becomes large, the inclusive cross-section and the 1-jet inclusive cross-section have independent perturbative expansions. This is because the dominant corrections to the first arise from terms of the form $\alpha_S C_A \pi$, while corrections to the second go like $\alpha_S \ln(m_{\mathrm{H}}/p_{\mathrm{T}}^{\mathrm{veto}})$, a quantity not present in the inclusive cross-section. Therefore, the scale variations for these two quantities should be considered independently. The uncertainty estimate for the 0-jet cross-section is then obtained by subtracting these two quantities and propagating errors in the standard fashion. The result of this procedure is shown in figure 7. The previous artificially small uncertainty estimate at low values of the jet cut is enhanced. Further evidence for the correctness of this increased error estimate is presented in ref. [21].

5. Conclusions

We have discussed several examples in which the interplay of experimental cuts and QCD corrections leads to surprising results. Corrections can be much larger than expected when experimental restrictions introduce a phase-space boundary. Such effects are very observable and process-dependent, and close interaction between theorists and experimenters is required to model the considered process correctly.

References

[1] https://twiki.cern.ch/twiki/bin/view/CMSPublic/PhysicsResultsEWK
[2] FERMILAB-CONF-12-065-E; CDF Note 10806; D0 Note 6303
[3] ATLAS-CONF-2012-019
[4] ATLAS Collaboration: G Aad *et al*, arXiv:1109.6572 [hep-ex]
[5] CMS Collaboration: S Chatrchyan *et al*, arXiv:1202.1489 [hep-ex]
[6] G Zanderighi, arXiv:1201.3905 [hep-ph]
[7] K Melnikov and F Petriello, *Phys. Rev.* **D74**, 114017 (2006), hep-ph/0609070
[8] R Gavin, Y Li, F Petriello and S Quackenbush, *Comput. Phys. Commun.* **182**, 2388 (2011), arXiv:1011.3540 [hep-ph]
[9] S Catani, L Cieri, G Ferrera, D de Florian and M Grazzini, *Phys. Rev. Lett.* **103**, 082001 (2009), arXiv:0903.2120 [hep-ph]
[10] G Balossini, G Montagna, C M Carloni Calame, M Moretti, O Nicrosini, F Piccinini, M Treccani and A Vicini, *J. High Energy Phys.* **1001**, 013 (2010), arXiv:0907.0276 [hep-ph]
[11] C Bernaciak and D Wackeroth, arXiv:1201.4804 [hep-ph]
[12] L Barze, G Montagna, P Nason, O Nicrosini and F Piccinini, arXiv:1202.0465 [hep-ph]
[13] CMS Collaboration: S Chatrchyan *et al*, *J. High Energy Phys.* **1110**, 007 (2011), arXiv:1108.0566 [hep-ex]
[14] S Frixione, P Nason and C Oleari, *J. High Energy Phys.* **0711**, 070 (2007), arXiv:0709.2092 [hep-ph]
[15] S Stoynev, private communication
[16] For example, see ATLAS Collaboration, arXiv:1202.1414 [hep-ex]
[17] J M Campbell, R K Ellis and C Williams, *J. High Energy Phys.* **1107**, 018 (2011), arXiv:1105.0020 [hep-ph]
[18] S Frixione and G Ridolfi, *Nucl. Phys.* **B507**, 315 (1997), hep-ph/9707345
[19] I W Stewart and F J Tackmann, *Phys. Rev.* **D85**, 034011 (2012), arXiv:1107.2117 [hep-ph]
[20] C Anastasiou, G Dissertori and F Stockli, *J. High Energy Phys.* **0709**, 018 (2007), arXiv:0707.2373 [hep-ph]
[21] S Dittmaier, S Dittmaier, C Mariotti, G Passarino, R Tanaka, S Alekhin, J Alwall, E A Bagnaschi *et al*, arXiv:1201.3084 [hep-ph]